

# Imprinted Polysilsesquioxanes for the Enhanced Recognition of Metal Ions

M. C. Burleigh,<sup>†,‡,§</sup> Sheng Dai,<sup>\*,†</sup> E. W. Hagaman,<sup>||</sup> and J. S. Lin<sup>⊥</sup>

Chemical Technology, Chemical and Analytical Sciences, and Solid State Divisions, Oak Ridge National Laboratory, P.O. Box 2008, Oak Ridge, Tennessee 37831-6181, and Department of Chemistry, University of Tennessee, Knoxville, Tennessee 37996-1600

Received November 14, 2000. Revised Manuscript Received April 25, 2001

Imprinting techniques have been used to synthesize organic–inorganic hybrid polymers with ionic recognition characteristics. 1,2-bis(trimethoxysilyl)ethane (BTSE) monomers were copolymerized with metal ion complexes of *N*-[3-(trimethoxysilyl)propyl]ethylenediamine ((TMS)en) in the presence of supramolecular assemblies of cetyltrimethylammonium chloride (CTAC), via room temperature, hydrolytic, sol–gel procedures. Subsequent extraction of the surfactant and metal ions results in a porous material with a high affinity for the metal ion template. Selective sorbents have been synthesized for Cu(II), Ni(II), and Zn(II). Adsorption studies indicate that these materials preferentially sequester the metal ion template from mixed solutions and exhibit fast uptake kinetics. These materials have been characterized by nitrogen gas adsorption, small-angle X-ray scattering, solid state <sup>13</sup>C NMR, and UV–visible spectroscopy.

## Introduction

The discovery of a new family of mesoporous silicon oxides (MCM-41) by scientists at Mobil Oil Research and Development<sup>1–5</sup> has led to great interest in this area of materials science. These materials exhibit large internal surface areas and narrow pore size distributions similar to those found in microporous crystalline zeolites. Unlike the crystalline zeolite materials with maximum pore dimensions < 20 Å, the pores of MCM-41 can be engineered with diameters from 15 to 100 Å. The relatively large pore sizes and ordered structures available make these materials very attractive for applications such as catalytic supports, sensors, and sorbents, especially when the molecules involved are too large to fit into the relatively small channels of conventional zeolites.

The synthesis of various MCM-41 type materials is based on a surfactant template approach. Surfactant molecules are used to form supramolecular assemblies in solution. These self-assembled structures act as templates for the formation of the porous matrix. Metal alkoxide precursors can undergo hydrolytic polymerization around these surfactant assemblies. Removal of the organic template via calcination or extraction effectively engineers the porosity of the resulting material. The final structure of the material depends on many factors such as surfactant chain length and charge, solution pH, and temperature. A wide variety of surfactants, including quaternary ammonium halides,<sup>6</sup> alkylamines,<sup>7,8</sup> poly(ethylene oxides),<sup>9</sup> and block copolymers,<sup>10</sup> have been used to synthesize porous materials in this manner.

Although it was initially used to synthesize metal oxides, the surfactant template approach is now used to engineer the porosity of a wide variety of new and novel materials. Hybrid porous materials have been synthesized by template-directed co-condensation of tetraalkoxysilanes and functional organotrialkoxysilanes.<sup>11–13</sup> Notably, Hall et al.<sup>11</sup> have demonstrated

\* To whom all correspondence should be addressed.

<sup>†</sup> Chemical Technology Division, Oak Ridge National Laboratory.

<sup>‡</sup> Department of Chemistry, University of Tennessee.

<sup>§</sup> Present address: Center for Bio/Molecular Science and Engineering, Naval Research Laboratory, Washington, DC 20375.

<sup>||</sup> Chemical and Analytical Sciences Division, Oak Ridge National Laboratory.

<sup>⊥</sup> Solid State Division, Oak Ridge National Laboratory.

(1) Kresge, C. T.; Leonowicz, M. E.; Roth, W. J.; Vartuli, J. C.; Beck, J. S. *Nature* **1992**, *359*, 710.

(2) Beck, J. S.; Vartuli, J. C.; Roth, W. J.; Leonowicz, M. E.; Kresge, C. T.; Schmitt, K. D.; Chu, C. T.; Olsen, D. H.; Sheppard, E. W.; McCullen, S. B.; Higgins, J. B.; Schlenker, J. L. *J. Am. Chem. Soc.* **1992**, *114*, 10834.

(3) Vartuli, J. C.; Schmitt, K. D.; Kresge, C. T.; Roth, W. J.; Leonowicz, M. E.; McCullen, S. B.; Hellring, S. D.; Beck, J. S.; Schlenker, J. L.; Olsen, D. H.; Sheppard, E. W. *Chem. Mater.* **1994**, *6*, 2317.

(4) Vartuli, J. C.; Kresge, C. T.; Leonowicz, M. E.; Chu, A. S.; McCullen, S. B.; Johnson, I. D.; Sheppard, E. W. *Chem. Mater.* **1994**, *6*, 2070.

(5) Beck, J. S.; Vartuli, J. C.; Kennedy, G. J.; Kresge, C. T.; Roth, W. J.; Schramm, S. E. *Chem. Mater.* **1994**, *6*, 1816.

(6) Huo, Q.; Margolese, D. I.; Stucky, G. D. *Chem. Mater.* **1996**, *8*, 1147.

(7) Bagshaw, S. A.; Prouzet, E.; Pinnavaia, T. J. *Science* **1995**, *269*, 1242.

(8) Bagshaw, S. A.; Pinnavaia, T. J. *Angew. Chem., Int. Ed. Engl.* **1996**, *35*, 1102.

(9) Prouzet, E.; Pinnavaia, T. J. *Angew. Chem., Int. Ed. Engl.* **1997**, *36*, 516.

(10) Zhao, D.; Huo, Q.; Feng, J.; Chmelka, B. F.; Stucky, G. D. *J. Am. Chem. Soc.* **1998**, *120*, 6024.

(11) Hall, S. R.; Fowler, C. E.; Lebeau, B.; Mann, S. *Chem. Commun.* **1999**, 201.

(12) Brown, J.; Mercier, L.; Pinnavaia, T. J. *Chem. Commun.* **1999**, 69.

that organo-functionalized MCM-41 silica hexagonal mesophases containing binary combinations of covalently linked phenyl, amino, or thiol moieties can be synthesized. The drawback associated with this methodology is that it is very difficult to increase the content of the functional organosilane without disrupting mesoporous silica networks. Accordingly, both surface areas and pore volumes of these materials decrease considerably with an increase of the functional organosilane content.

Recently, Inagaki et al.<sup>14</sup> have developed a novel methodology to synthesize porous hybrid materials based on the sol-gel processing of a single bridged-silsesquioxane precursor. No tetraalkoxysilanes were employed in these reactions. Highly porous and periodic organosilicas with organic groups inside the channel walls were synthesized. The key to the success of this new synthetic methodology lies in the unique structural feature of the bridged silsesquioxane sol-gel precursor. The organic moiety in these hybrid materials is part of the cross-linked network and not simply a side chain. The organic portion of the sol-gel precursor functions as a rigid bridge between two alkoxy-silyl groups through covalent carbon-silicon bonds. A variety of these bridged silsesquioxane sol-gel precursors have been previously synthesized with bridges containing a wide variety of organic groups.<sup>15-19</sup> The use of a single precursor allows the organic-inorganic ratio to be fixed. More recently, Stein and co-workers<sup>20</sup> reported the synthesis of similar ordered materials by using both 1,2-bis(triethoxysilyl)ethane and 1,2-bis(triethoxysilyl)ethylene and cetyltrimethylammonium bromide (CTAB) surfactant. The ethyl-bridged material exhibited better hydrothermal stability than a pure silica MCM-41 sample. Ozin and co-workers<sup>21</sup> compared the properties of mesoporous organic-inorganic polymers that were synthesized using various ratios of 1,2-bis(triethoxysilyl)ethylene and tetraethyl orthosilicate, to CTAB surfactant.

We have been interested in exploring mesoporous materials as hosts for molecular imprinting.<sup>27b-32</sup> The technique of molecular imprinting involves the incor-

poration of a template into a host matrix by combining it with host monomers that polymerize around the template. Subsequent removal of the template results in a material that contains imprint cavities with a favorable size, shape, and chemical environment to selectively rebinding the template. The imprinting approach based on organic polymer hosts was first developed by Wulff and Sarhan<sup>22</sup> who used this technique to produce polymers for the resolution of racemic mixtures. It has since been utilized in the development of artificial enzymes<sup>23</sup> and antibodies,<sup>24,25</sup> chromatographic resins,<sup>26</sup> and metal ion sorbents.<sup>25a,c,27</sup>

Herein, we report a new approach for the synthesis of ion-imprinted sorbents based on the newly developed mesoporous polysilsesquioxane. The mesoporous polysilsesquioxane is used here as a host matrix for functional organosilane ligands or their complexes with target metal ions. The structural similarities between bridged silsesquioxanes and organosilanes allow a good mixing of these sol-gel precursors and a uniform incorporation of the functional ligands into the mesoporous silsesquioxane framework. Accordingly, relatively high concentrations of the functional ligand can be incorporated into mesoporous hosts without disrupting the mesoporous network. The bridged silsesquioxane used in this investigation, 1,2-bis(triethoxysilyl)ethane (BTSE), can generate very stable and ordered mesophases of organosilicas. Briefly, copolymerization of BTSE with metal ion complexes of N-[3-(trimethoxysilyl)propyl]ethylenediamine ((TMS)en) around supramolecular assemblies of cetyltrimethylammonium chloride (CTAC) gives a composite polymer. Extraction of the surfactant and metal ions results in a porous material with a high affinity for the metal ion template. Both the metal ions and the surfactant micelles act as templates in this system. Removal of the surfactant leaves a network of pore channels that give these sorbents large surface areas and excellent metal ion transfer kinetics. Removal of the metal ions results in the formation of tailored binding sites made up of ethylenediamine functionalities that are arranged in conformations that favor rebinding to the metal ion template. Selective sorbents have been synthesized for Cu(II), Ni(II), and Zn(II).

## Experimental Section

**Chemicals.** 1,2-Bis(triethoxysilyl)ethane (BTSE) and N-[3-(trimethoxysilyl)propyl]ethylenediamine ((TMS)en) were obtained from Gelest, Inc.; sodium hydroxide (50 wt %) and cetyltrimethylammonium chloride (CTAC) 25 wt % were obtained from Aldrich. The nitrate salts of copper, nickel, zinc, and cadmium were purchased from Fluka. Nitric acid (69%) and hydrochloric acid (37%) were obtained from J. T. Baker. The absolute ethyl alcohol was purchased from AAPER Alcohol and Chemical. All chemicals were used as received.

**Synthesis.** The BTSE monomer undergoes polymerization by base-catalyzed hydrolysis and condensation reactions, as shown in steps 1 and 2 (Scheme 1).

(13) (a) Lim, M. L.; Blanford, C. F.; Stein, A. *J. Am. Chem. Soc.* **1997**, *119*, 4090. (b) Stein, A.; Melde, B. J.; Schroden, R. C. *Adv. Mater.* **2000**, *12*, 1403.

(14) Inagaki, S.; Guan, S.; Fukushima, Y.; Ohsuna, T.; Terasaki, O. *J. Am. Chem. Soc.* **1999**, *121*, 9611.

(15) Loy, D. A.; Shea, K. J. *Chem. Rev.* **1995**, *95*, 1431.

(16) Shea, K. J.; Loy, D. A. *Chem. Mater.* **1989**, *1*, 572.

(17) Corriu, R. J. P. *Angew. Chem., Int. Ed. Engl.* **2000**, *39*, 1376.

(18) Corriu, R. J. P.; Leclercq, D. *Angew. Chem., Int. Ed. Engl.* **1996**, *35*, 1420.

(19) Cerveau, G.; Corriu, R. J. P. *Coord. Chem. Rev.* **1998**, *178-80*, 1051.

(20) Melde, B. J.; Holland, B. T.; Blanford, C. F.; Stein, A. *Chem. Mater.* **1999**, *11*, 3302.

(21) Asefa, T.; MacLachlan, M. J.; Coombs, N.; Ozin, G. A. *Nature* **1999**, *402*, 867.

(22) Wulff, G.; Sarhan, A. *Angew. Chem., Int. Ed. Engl.* **1972**, *11*, 341.

(23) Mosbach, K. *Trends Biochem. Sci.* **1994**, *19*, 9.

(24) (a) Shea, K. J. *Trends Polym. Sci.* **1994**, *2*, 166. (b) J. Mathew-Krotz, K. J. Shea, *J. Am. Chem. Soc.* **1996**, *118*, 8154.

(25) (a) Wulff, G. *Angew. Chem., Int. Ed. Engl.* **1995**, *34*, 1812. (b) Sellergren, B. *Angew. Chem., Int. Ed. Engl.* **2000**, *39*, 1031. (c) Steinke, J.; Sherrington, D. C.; Dunkin, I. R. *Adv. Polym. Sci.* **1995**, *123*, 81.

(26) Takeuchi, T.; Matsui, J. *Acta Polym.* **1996**, *47*, 471.

(27) (a) *Molecular and Ionic Recognition with Imprinted Polymers*; Bartsch, R. A., Maeda, M., Ed.; American Chemical Society: Washington, DC, 1998. (b) Dai, S.; Burleigh, M. C.; Shin, Y.; Morrow, C. C.; Barnes, C. E.; Xue, Z. L. *Angew. Chem., Int. Ed. Engl.* **1999**, *38*, 1235.

(28) Dai, S.; Shin, Y. S.; Barnes, C. E.; Toth, L. M. *Chem. Mater.* **1997**, *9*, 2521.

(29) Dai, S.; Shin, Y. S.; Ju, Y. H.; Burleigh, M. C.; Lin, J. S.; Barnes, C. E.; Xue, Z. L. *Adv. Mater.* **1999**, *11*, 1226.

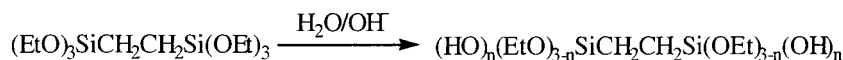
(30) Dai, S.; Ju, Y. H.; Burleigh, M. C.; Gao, H. J.; Lin, J. S.; Pennycook, S.; Barnes, C. E.; Xue, Z. L. *J. Am. Chem. Soc.* **2000**, *122*, 992.

(31) Burleigh, M. C.; Dai, S.; Hagaman, C. E.; Xue, Z. L. *Separ. Sci. Tech.*, in press.

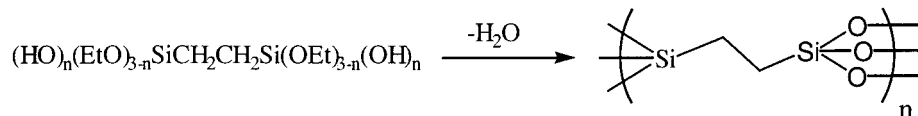
(32) Burleigh, M. C.; Dai, S.; Hagaman, E. W.; Barnes, C. E.; Xue, Z. L. *ACS Symp. Ser.* **2001**, *778*, 146.

## Scheme 1

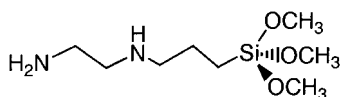
(1) Base catalyzed Hydrolysis:



(2) Condensation:



**Functionalization.** The polymer is functionalized by incorporation of the bifunctional reagent, TMSen, into the reaction mixture.



The methoxy groups of (TMS)en readily undergo hydrolysis and condensation reactions, which anchor it to the polymer. The ethylenediamine moiety contains nitrogen donor atoms that can sequester metal ions from aqueous solutions by forming stable complexes via dative bonding.

The hybrid materials in this study were synthesized according to the following procedures.

**Blank Hybrid.** The appropriate amount of 25% (w/w) cetyltrimethylammonium chloride solution was added to deionized water. Sodium hydroxide was added upon stirring, followed by the addition of BTSE. The resulting reaction mixture had the following molar composition: 1.0:0.12:1.0:230 BTSE:CTAC:NaOH:H<sub>2</sub>O.

The reaction mixture was stirred in a closed vessel at room temperature for 24 h, and the solid precipitate was recovered via vacuum filtration.

**Nonimprinted Hybrid.** A protocol similar to that of the blank hybrid was used, with the addition of the bifunctional ligand, TMSen, after the BTSE. The molar composition of the reaction mixture was 1.0:0.12:0.15:1.0:230 BTSE:CTAC:(TMS)en:NaOH:H<sub>2</sub>O.

**Copper Imprinted Hybrid.** The appropriate amount of 25 wt % cetyltrimethylammonium chloride solution was added to deionized water. Cu(NO<sub>3</sub>)<sub>2</sub>·3H<sub>2</sub>O was then dissolved in the micellar solution. (TMS)en was then added while stirring, followed by the BTSE. NaOH was then added to the reaction mixture, which had the following molar composition: 1.0:0.12:0.15:0.075:1.0:230 BTSE:CTAC:(TMS)en:Cu(NO<sub>3</sub>)<sub>2</sub>·3H<sub>2</sub>O:NaOH:H<sub>2</sub>O.

**Nickel and Zinc Imprinted Hybrids.** A procedure similar to that described above for the copper imprinted material was followed, except that the amount of metal salt used [Ni(NO<sub>3</sub>)<sub>2</sub>·6H<sub>2</sub>O or Zn(NO<sub>3</sub>)<sub>2</sub>·6H<sub>2</sub>O] was decreased, so that the (TMS)en:metal ion molar ratio was 3:1. This resulted in the following reaction mixture molar ratios: 1.0:0.12:0.15:0.05:1.0:230 BTSE:CTAC:(TMS)en:M<sup>II</sup>(NO<sub>3</sub>)<sub>2</sub>·3H<sub>2</sub>O:NaOH:H<sub>2</sub>O.

**Postsynthetic Processing.** After recovery via vacuum filtration, the solid precipitates were rinsed with deionized water and ethanol and placed under vacuum at 80 °C for 4 h. At this point, the materials are dubbed "as-synthesized", and the appropriate amounts needed for characterization were removed. The remaining material was placed in excess 1.0 M HNO<sub>3</sub> and stirred for 15 min. This material was recovered by vacuum filtration, rinsed with deionized water, and placed in a large excess (~150 mL/g) of EtOH/HCl (1.0 M wrt HCl). This mixture was stirred well under gentle heating (50 °C) for 8 h. The sorbent is again recovered by vacuum filtration, washed with plenty of EtOH, and dried under vacuum at 80 °C for 1 h.

**Batch Procedures.** All metal ion solutions were buffered to a specific pH with sodium acetate/acetic acid (0.05 M). In a typical run, 0.1 g of sorbent and 10 mL of metal ion solution were placed in capped PET vials and sonicated for 30 min. The resulting mixture was filtered, and both the filtrate and the initial standard solutions were analyzed via ICP/OES spectroscopy in order to measure the initial and final metal ion concentrations. The overall capacity of the sorbent for a given metal ion was then calculated by the change in concentration between the filtrate and the initial metal ion solution.

**Analytical Techniques.** All metal ion concentration analyses were performed with a Thermo Jarrel Ash Iris inductively coupled plasma spectrometer. Nitrogen adsorption isotherms were measured with a Micromeritics Gemini 2375 surface area analyzer. UV/visible spectra were measured with a Cary 14H scanning spectrophotometer converted by On-Line Instrument Systems (OLIS) for data acquisition via PC. <sup>13</sup>C NMR spectra were recorded with a Bruker MSL 100 spectrometer operating at 2.35 T. X-ray scattering plots of the hybrid samples were measured with the 10 m small-angle X-ray scattering camera at the SAXS user facility of the Oak Ridge National Laboratory.

## Results and Discussion

**Metal Ion Sorption.** *Metal(II) Uptake Capacity.* The metal ion imprinted hybrids exhibit an enhanced capacity relative to the nonimprinted material for the adsorption of metal ions from aqueous solutions. The ability of a sorbent to remove a given ion from solution can be expressed in terms of a distribution constant ( $K_d$ ),

$$K_d = \left\{ \frac{(C_0 - C_f)}{C_f} \right\} \left\{ \frac{\text{solution volume (mL)}}{\text{mass sorbent (g)}} \right\} \quad (1)$$

where  $C_0$  and  $C_f$  are the initial and final concentrations of the given ion in solution.

**Copper(II) Imprinted Hybrids.** Plots of the logarithm of the distribution coefficient versus initial Cu(II) concentration are shown in Figure 1 for the copper imprinted and nonimprinted hybrid materials from solutions ranging from 6.35 to 63.55 ppm Cu(II) during a standard batch procedure at pH 5.0. A direct comparison shows that the copper imprinted material removed more of the copper ions than the nonimprinted hybrid at every concentration. This is a clear example of the increased affinity of the imprinted sorbent for the metal ion template. More than a 10-fold increase in the distribution coefficients is achieved by the molecular imprinting technique.

**Nickel(II) Imprinted Hybrids.** Unlike the Cu(II) ion, which generally forms a 1:2 metal to ligand complex with the ethylenediamine moiety, the Ni(II) ion preferentially forms a 1:3 complex, resulting in an octahedral

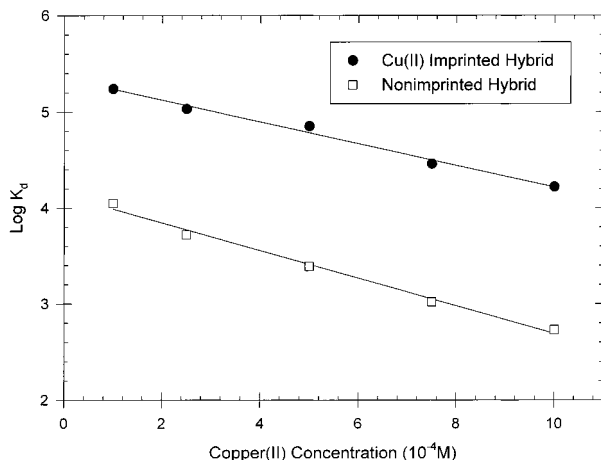


**Figure 1.** Cu(II) adsorption isotherms for the copper imprinted and nonimprinted sol-gels. Solutions were buffered at pH = 5.0 with HAc/NaAc (0.05 M). A 0.1 g amount of sorbent was equilibrated with 10 mL of metal ion solution for 1 h.

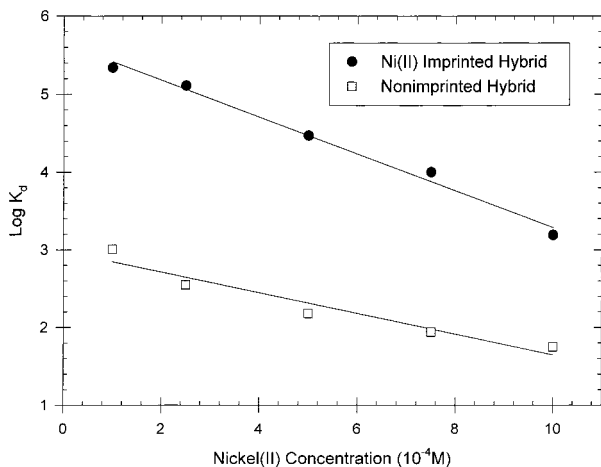


**Figure 2.** Ni(II) adsorption isotherms for the nickel imprinted and nonimprinted sol-gels. Solutions were buffered at pH = 5.0 with HAc/NaAc (0.05 M). A 0.1 g amount of sorbent was equilibrated with 10 mL of metal ion solution for 1 h.

coordination environment, where the metal ion is surrounded by six nitrogen donor atoms.<sup>33</sup> For this reason, we altered the reaction mixture stoichiometry from that used for the Cu(II) imprinted hybrid by reducing the molar ratio of the nitrate salt used, thereby forming the 1:3 Ni(II):en complex. The resulting imprinted material should contain binding sites tailored for this cation. Figure 2 shows the logarithm of the distribution coefficient versus initial Ni(II) concentration exhibited by both nickel imprinted and nonimprinted hybrids during standard batch tests at pH 6.0. The nickel imprinted sorbent removed more Ni(II) than the nonimprinted sorbent at all concentrations. The increase in the Ni(II) distribution coefficients as a result of molecular imprinting is evident.

**Zinc(II) Imprinted Hybrids.** The synthetic procedure for the Zn(II) imprinted hybrid material was similar to that of the nickel imprinted hybrid, since it also preferentially forms a 1:3 complex with the ethylenediamine moiety. Figure 3 shows the logarithm of the distribution coefficient versus initial Zn(II) concentra-

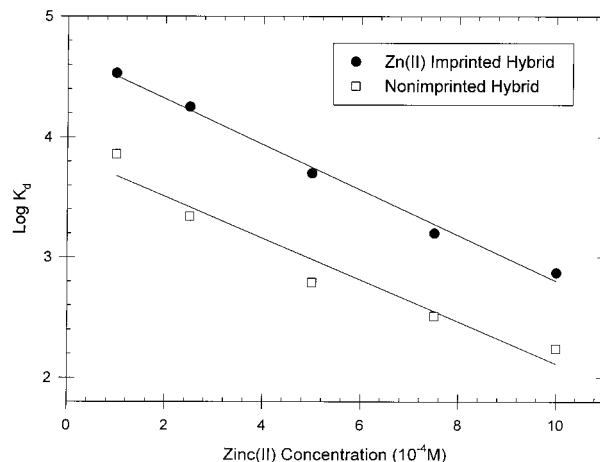
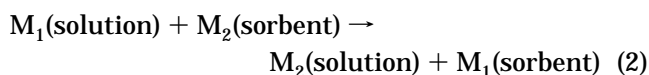


**Figure 3.** Zn(II) adsorption isotherms for the zinc imprinted and nonimprinted sol-gels. Solutions were buffered at pH = 5.0 with HAc/NaAc (0.05 M). A 0.1 g amount of sorbent was equilibrated with 10 mL of metal ion solution for 1 h.

tion exhibited by both the zinc imprinted and nonimprinted hybrid materials from solutions ranging from 6.54 to 65.39 ppm Zn(II) during a standard batch procedure at pH 6.0. Not unlike the copper and nickel imprinted sorbents, the zinc imprinted hybrid removed more Zn(II) than the nonimprinted material at all concentrations studied.

**Metal(II) Selectivity.** Although the results of the single metal ion batch tests described above clearly illustrate how molecular imprinting techniques can be utilized to create materials which exhibit enhanced recognition for specific metal ions, the vast majority of metal ion sorbent applications require selective separations. Therefore, the sorbent must be able to selectively bind the metal ion of choice from a mixture that contains various competitor species. A selectivity coefficient,  $k$ , for the binding of a specific metal ion in the presence of competitor species can be obtained from equilibrium binding data according to eq 3:



$$k = \frac{\{[M_2]_{\text{solution}}[M_1]_{\text{sorbent}}\}}{\{[M_1]_{\text{solution}}[M_2]_{\text{sorbent}}\}} = \frac{K_d(M_1)}{K_d(M_2)} \quad (3)$$

A comparison of the  $k$  values for the imprinted and nonimprinted samples can show the effect that imprinting has on the metal ion selectivity for a given sorbent.<sup>34</sup> A measure of the increase in selectivity due to molecular imprinting can be defined by the ratio of the selectivity coefficients of the imprinted and nonimprinted materials and is referred to as the relative selectivity coefficient,  $k'$ .

$$k' = k_{\text{imprinted}}/k_{\text{nonimprinted}} \quad (4)$$

**Cu(II) vs Zn(II) Selectivity.** To test the selectivity of the copper imprinted hybrid sorbents, competitive ion binding batch studies were undertaken, with Zn(II) as the competitor species. All standard solutions were

(33) Cotton, F. A.; Wilkinson, G.; Murillo, C. A.; Bochmann, M. *Advanced Inorganic Chemistry*, 6th ed.; Wiley: New York, 1999.

(34) Kuchen, W.; Schram, J. *Angew. Chem., Int. Ed. Engl.* **1988**, *27*, 1695.

**Table 1. Competitive Loading of  $M_1(\text{Cu}^{2+})$  and  $M_2(\text{Zn}^{2+})$  by Copper Imprinted and Control Blank Samples at pH 5.0 (HAc/NaAc Buffer)**

sorbent	$C_0(\text{Cu/Zn})$ (M)	% abs		$K_d$		$k$	$K$
		Cu	Zn	copper	zinc		
Nimp <sup>a</sup>	$10^{-4}$	98.99	20.20	9 700	25.3	386	
Cu-imp <sup>b</sup>	$10^{-4}$	99.93	85.47	153 000	588	260	0.67
Nimp	$2.5 \times 10^{-4}$	96.60	20.08	2 840	25.1	113	
Cu-imp	$2.5 \times 10^{-4}$	99.92	74.68	129 700	295	440	3.9
Nimp	$5.0 \times 10^{-4}$	92.69	14.33	1 270	16.7	76	
Cu-imp	$5.0 \times 10^{-4}$	99.88	60.38	85 400	152.4	561	7.4
Nimp	$7.5 \times 10^{-4}$	89.81	6.71	880	7.2	122	
Cu-imp	$7.5 \times 10^{-4}$	99.80	43.63	48 800	77.4	631	5.2
Nimp	$10^{-3}$	80.84	4.30	420	4.5	94	
Cu-imp	$10^{-3}$	99.58	31.62	23 500	46	507	5.4

<sup>a</sup> Nimp: nonimprinted sorbent. <sup>b</sup> Cu-imp: copper-imprinted sorbent.

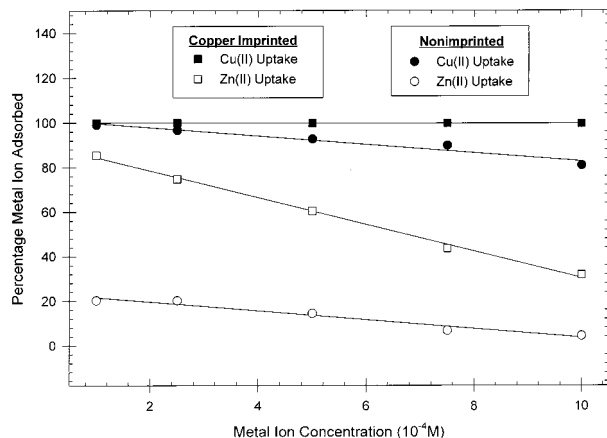


**Figure 4.**  $\text{Cu}^{2+}$  and  $\text{Zn}^{2+}$  uptake by the copper imprinted and nonimprinted sorbents in the pH range 3.0–5.5, buffered with HAc/NaAc (0.05 M). All solutions were  $5 \times 10^{-3}$  wrt both copper and zinc.

made with equimolar amounts of  $\text{Cu}(\text{II})$  and  $\text{Zn}(\text{II})$  at five different concentrations from  $10^{-4}$  to  $10^{-3}$  M (wrt both ions) and pH 5.0. Identical tests were run with the nonimprinted hybrid sorbent for comparison. The results of competitive ion binding batch tests are summarized in Table 1. The nonimprinted sorbent absorbed more  $\text{Cu}(\text{II})$  than  $\text{Zn}(\text{II})$  at all concentrations. This is an expected result, due to the larger stability constants associated with the formation of ethylenediamine: copper complexes relative to those of zinc at pH 5.0. The copper imprinted hybrid absorbed more  $\text{Cu}(\text{II})$  and more  $\text{Zn}(\text{II})$  than the nonimprinted material at all concentrations. The enhanced capacity of  $\text{Cu}(\text{II})$  due to molecular imprinting is expected, while the increased uptake of the  $\text{Zn}(\text{II})$  competitor species is less clear. The imprinting seems to create electron-rich, hydrophilic sites in the relatively hydrophobic organic–inorganic matrix. These sites may increase the sorbent's affinity for a wide variety of hydrated metal ions. An important concept here is that the imprinting enhances the affinity of the sorbent for the target  $\text{Cu}(\text{II})$  more than that of the  $\text{Zn}(\text{II})$  competitor. This is shown by the larger selectivity coefficients,  $k$ , and relative selectivity coefficients,  $K$ , greater than unity for the copper imprinted sorbent at all solution concentrations with the exception of the lowest ( $10^{-4}$ : $10^{-4}$   $\text{Cu}(\text{II})$ : $\text{Zn}(\text{II})$ ). At this low concentration the imprinted material has enough binding sites to remove most of both metal species, decreasing its calculated selectivity. Figure 4 shows a larger increase in the distribution coefficients for  $\text{Cu}(\text{II})$  relative to

**Table 2.  $\text{Cu}(\text{II})/\text{Zn}(\text{II})$  Selectivity**

sorbent <sup>a</sup>	$C_0(\text{Cu})$ (ppm)	$C_f(\text{Cu})$ (ppb)	$C_0(\text{Zn})$ (ppm)	$C_f(\text{Zn})$ (ppb)	$C_f(\text{Zn})/C_f(\text{Cu})$
Nimp	6.35	64	6.54	5 220	81.6
Cu-imp	6.35	4	6.54	950	238
Nimp	15.89	540	16.35	13 070	24.2
Cu-imp	15.89	13	16.35	4 140	318
Nimp	31.77	2,320	32.70	28 010	12.1
Cu-imp	31.77	38	32.70	12 960	341
Nimp	47.66	4 860	49.04	45 750	9.4
Cu-imp	47.66	95	49.04	27 640	291
Nimp	63.55	12 180	65.39	62 580	5.1
Cu-imp	63.55	267	65.39	44 710	167

<sup>a</sup> See abbreviation definitions in Table 1 footnotes *a* and *b*.

$\text{Zn}(\text{II})$  for the copper imprinted material than the nonimprinted sorbent. Although the nonimprinted material removes nearly all the  $\text{Cu}(\text{II})$  and only about 20% of the  $\text{Zn}(\text{II})$  at the lowest concentration, both values decrease approximately the same amount (17%) over the entire concentration range. This is not the case with the metal ion sorption trend of the  $\text{Cu}(\text{II})$  imprinted material. At the higher concentrations, where the competition for adsorption sites is high, the percentage of the  $\text{Cu}(\text{II})$  adsorbed remains over 99.5%, while the percentage of the  $\text{Zn}(\text{II})$  competitor decreases substantially.

Another way to describe the selectivity of a given sorbent for a target metal ion over a competitor species is simply the ratio between the final concentrations of the two species. In this instance, the larger the value of  $C_f(\text{Zn}(\text{II})):C_f(\text{Cu}(\text{II}))$ , the higher the selectivity of the sorbent for  $\text{Cu}(\text{II})$ . Table 2 shows that the value of this ratio is considerably higher for the copper imprinted sorbent at all concentrations.

*Ni(II) vs Zn(II) Selectivity.* The selectivities of the nickel and zinc imprinted sorbents were investigated by competitive ion binding batch tests. All initial solutions contained equimolar amounts of  $\text{Ni}(\text{II})$  and  $\text{Zn}(\text{II})$  at five different concentrations from  $10^{-4}$  to  $10^{-3}$  M (wrt both ions) and pH 6.0. Table 3 summarizes the batch test results. The nickel imprinted sorbent absorbed more  $\text{Ni}(\text{II})$  than  $\text{Zn}(\text{II})$  at all concentrations. This results in higher distribution coefficients for  $\text{Ni}(\text{II})$  than  $\text{Zn}(\text{II})$  with the nickel imprinted material. This sorbent removed nearly all of both metal ion species from the  $10^{-4}$  M: $10^{-4}$  M  $\text{Ni}(\text{II})$ : $\text{Zn}(\text{II})$  mixed solution. This lack of selectivity at very low concentrations may be due to the high number of imprinted sites relative to the total number of metal ions. In direct contrast to the adsorption behavior of the nickel imprinted material, the zinc imprinted sorbent absorbed more  $\text{Zn}(\text{II})$  than  $\text{Ni}(\text{II})$  at

**Table 3. Competitive Loading of  $M_1(Ni^{2+})$  and  $M_2(Zn^{2+})$  by Nickel Imprinted and Zinc Imprinted Sorbents at pH 5.0 (HAc/NaAc Buffer)**

sorbent <sup>a</sup>	$C_0(Ni)$ (ppm)	$C_f(Ni)$ (ppb)	% Ni abs	$C_0(Zn)$ (ppm)	$C_f(Zn)$ (ppb)	% Zn abs	Ni $K_d$	Zn $K_d$
Ni-imp	5.87	5	99.92	6.54	6	99.91	126 800	116,600
Zn-imp	5.87	29	99.50	6.54	1.3	99.98	20 100	411 200
Ni-imp	14.67	16	99.89	16.35	26	99.84	90 100	61 000
Zn-imp	14.67	293	98.00	16.35	20	99.88	4 900	82 500
Ni-imp	29.35	360	98.77	32.70	1 000	96.90	8 000	3 100
Zn-imp	29.35	4 300	85.44	32.70	481	98.53	590	6 700
Ni-imp	44.02	3 120	92.91	49.04	6 560	86.62	1 300	650
Zn-imp	44.02	16 380	62.80	49.04	3 710	92.43	170	1 200
Ni-imp	58.69	9 180	84.35	65.39	17 700	72.88	540	270
Zn-imp	58.69	32 100	45.30	65.39	11 490	82.43	83	470

<sup>a</sup> See abbreviation definitions in Table 1 footnotes *a* and *b*.

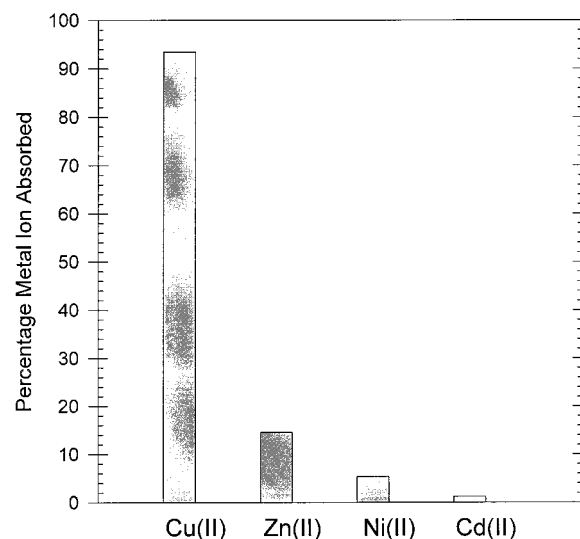


**Figure 5.** Metal ion uptakes of a divalent cation mixture by copper imprinted sorbent.

all concentrations studied. This results in higher distribution coefficients for Zn(II) than Ni(II) with the zinc imprinted material. This illustration of reversible imprinting shows the utility of imprinting techniques in the synthesis selective metal ion sorbents.

**Divalent Cation Mixture.** The divalent cations of copper, nickel, zinc, and cadmium are common constituents of man-made waste. They are often present together in municipal wastewater, electroplating waste, acid mine drainage, and landfill leachates.<sup>35–37</sup> To determine the adsorption selectivity characteristics of the copper imprinted hybrid sorbent in these complex matrices, a metal ion solution,  $10^{-3}$  M with respect to Cu(II), Ni(II), Zn(II), and Cd(II), was prepared at pH 5.0 and used as a waste simulant. The results of a batch test with the copper imprinted sorbent are shown in Figure 5. Over 93% of the copper was absorbed, while the amount of zinc, nickel, and cadmium absorbed was approximately 15, 5, and 1%, respectively.

**Adsorption Kinetics.** A very important attribute of any sorbent is the time required for the absorption process to take place. Many potential applications, such as product or waste stream purification, require relatively fast uptake kinetics for any sorbent technology to be a viable option. The copper absorption study

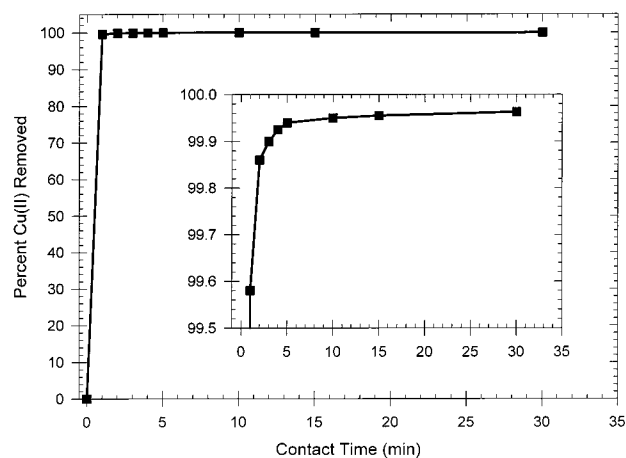


**Figure 6.** Percent copper absorbed from  $10^{-4}$  M solution (pH = 5.0) versus contact time for the copper imprinted sol-gel. A 0.1 g amount of sorbent was placed in 10 mL of metal ion solution for each data point.

(Figure 1) showed that 0.1 g of the copper imprinted sorbent removed over 99.8% of the copper from 10 mL of a  $5 \times 10^{-4}$  M solution at pH 5.0. Since all the batch tests involved a 30 min contact time, a series of tests were run with lower contact times in order to deduce how fast the adsorption process occurs in the organic-inorganic matrix. Figure 6 illustrates the adsorption percentage as a function of the contact time. The copper imprinted hybrid removed over 99.5% of the Cu(II) during the first minute. During this time the initial copper concentration (31.77 ppm) is reduced to 130 ppb.

**Multiple Use Cycles.** One factor which determines the economic feasibility of any sorbent is the ease by which it can be regenerated. The ability to recycle a sorbent can offset initial costs. A series of Cu(II) batch experiments were carried out with the copper imprinted and nonimprinted sorbents in which copper-loaded sorbents were washed with 1 M  $HNO_3$  to remove the metal ions, neutralized, and used again. These multiple use cycles were used in order to determine a number of key factors, such as the ability of the acid to remove the metal ions and whether the sorbents would retain their Cu(II) uptake capacities after numerous cycles. In a typical run, 0.50 g of sorbent was placed in 50 mL of  $5 \times 10^{-4}$  M Cu(II) solution and sonicated for 30 min. The sorbent was then recovered by filtration and placed in 10 mL of 1 M  $HNO_3$ , stirred for 5 min, and then recovered by vacuum filtration. The sorbent was then placed in 50 mL of deionized water and titrated to neutral pH with 1 M NaOH. Following another filtration step, the sorbents were dried, weighed, and reused. Due

(35) Banks, D.; Younger, P. L.; Arnesen, R. T.; Iversen, E. R.; Banks, S. B. *Environ. Geol.* **1997**, *32*, 157.

(36) Mantei, E. J.; Sappington, E. J. *Environ. Geol.* **1994**, *24*, 287.

(37) Brower, J. B.; Ryan, R. L.; Pazirandeh, M. *Environ. Sci. Technol.* **1997**, *31*, 2910.

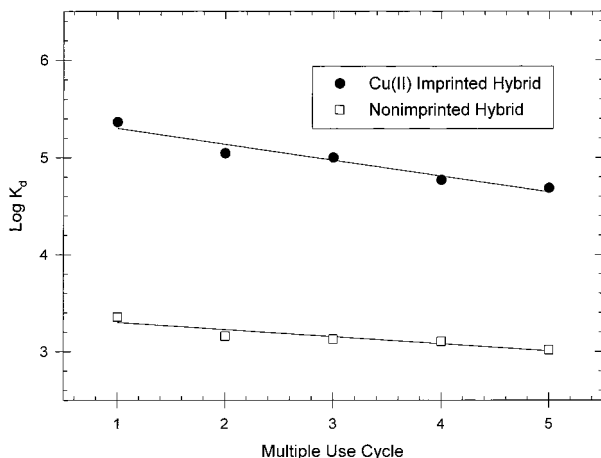


**Figure 7.** Multiple use recycles of copper imprinted and nonimprinted sorbents.

to the number of steps involved, approximately 5% of the total mass of the sorbents was lost during each cycle. The amount of the initial Cu(II) solution was adjusted (i.e. 0.485 g/48.50 mL) to take this into account. These procedures were then repeated four more times. Figure 7 shows the values of the distribution coefficients for both the copper imprinted and nonimprinted sorbents for five multiple use cycles. A slight decrease in  $K_d$  is shown by both sorbents for each successive use. Despite this small decrease, the copper imprinted hybrid removed greater than 99.70% of the Cu(II) during the fifth and final cycle. Filtrate analyses show that the simple acid washing removed greater than 98% of the Cu(II) from the loaded sorbents.

**Small-Angle X-ray Scattering.** Small-angle X-ray scattering plots of both the as-synthesized and extracted samples of the blank, nonimprinted, and copper imprinted hybrid materials are shown in Figure 8. All samples exhibit single  $d_{100}$  reflections. Higher order Bragg reflections are not resolved. The extracted samples exhibit a much higher intensity due to the larger change in electron densities caused by removal of the surfactant assemblies. The as-synthesized materials, which still contain CTAC, show much lower intensities. The remarkable similarity of all three extracted samples seems to indicate that incorporation of (TMS)en into the nonimprinted sorbent and copper:(TMS)en complexes into the copper imprinted sorbent does not diminish the local order in these materials. Furthermore, these plots show very little change in the location of the  $d_{100}$  reflection due to the removal of the surfactant template and, therefore, no evidence of any collapse of the porous network during extraction. The presence of copper in the copper imprinted as-synthesized material may account for the inconsistencies shown by this plot. Values of the structural parameters  $Q_{\max}$ ,  $\lambda_{\max}$ ,  $d_{100}$ , and  $a_0$  are listed in Table 4. Although no reflections higher than  $d_{100}$  have been resolved, Pinnavaia and co-workers have shown that similar single reflection materials can still exhibit local hexagonal symmetry.<sup>38,39</sup>

**Nitrogen Adsorption.** Following the postsynthetic processing, a nitrogen adsorption analysis was per-

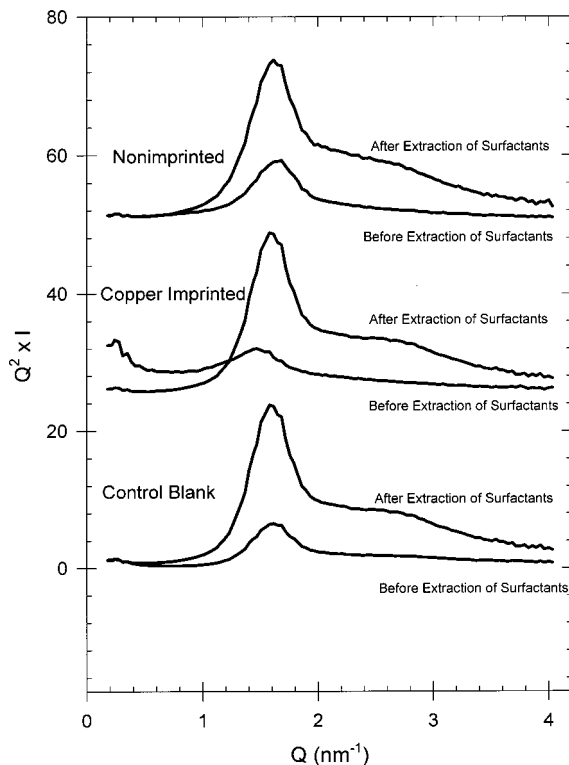


**Figure 8.** SAXS patterns of hybrid sorbents.

**Table 4. SAXS Data for Hybrid Sorbents**

sample	$Q_{\max}$ (nm <sup>-1</sup> )	$2\Theta_{\max}$ (deg)	$d_{100}$ (Å)	$a_0$ (Å)
blank as-synthesized	1.614	2.266	38.93	44.95
blank extracted	1.580	2.219	39.77	45.92
nonimprinted as-synthesized	1.649	2.316	38.10	43.99
nonimprinted extracted	1.614	2.266	38.93	44.95
Cu imprinted as-synthesized	1.469	2.063	42.77	49.39
Cu imprinted extracted	1.505	2.114	41.75	48.21

formed on each sample. Figure 9 shows the nitrogen adsorption isotherms for the metal ion imprinted, non-imprinted, and blank hybrid sorbents after postsynthetic processing. All sorbents exhibit type I isotherms,<sup>40</sup> indicating a microporous structure. Linear regions from  $P/P_0 = 0.1-0.3$  indicate supermicroporosity.<sup>41</sup> Table 5 contains the porosity data of the extracted hybrid sorbents. Surface areas were obtained using the BET method.<sup>42</sup> The total pore volumes of the hybrid samples simply represent the volume of the liquid equivalent of the total nitrogen absorbed. Micropore surface areas and micropore volumes were calculated by using the  $t$ -method.<sup>43</sup> The  $d$  spacings were calculated from small-angle X-ray scattering data, assuming a local hexagonal packing of the mesopores. All sorbents exhibit large surface areas and pore volumes. Another distinguishing feature of these materials is the rather large micropore volumes. Typical BJH pore size distributions,<sup>44</sup> of these materials indicate that the few mesopores present in these samples are  $\sim 20$  Å. The large micropore volumes

(40) Brunauer, S.; Deming, L. S.; Deming, W. S.; Teller, E. *J. Am. Chem. Soc.* **1940**, *62*, 1723.

(41) Gregg, S. J.; Sing, K. S. W. *Adsorption, Surface Area, and Porosity*, 2nd ed.; Academic Press: New York, 1983.

(42) Brunauer, S.; Emmett, P. H.; Teller, E. *J. Am. Chem. Soc.* **1938**, *60*, 309.

(43) Lippens, B. C.; De Boer, J. H. *J. Catal.* **1965**, *4*, 319.

(44) Barrett, E. P.; Joyner, L. G.; Halenda, P. P. *J. Am. Chem. Soc.* **1951**, *73*, 373.

(38) Tanev, P. T.; Chibwe, M.; Pinnavaia, T. J. *Nature* **1994**, *368*, 321.

(39) Tanev, P. T.; Pinnavaia, T. J. *Science* **1995**, *267*, 865.

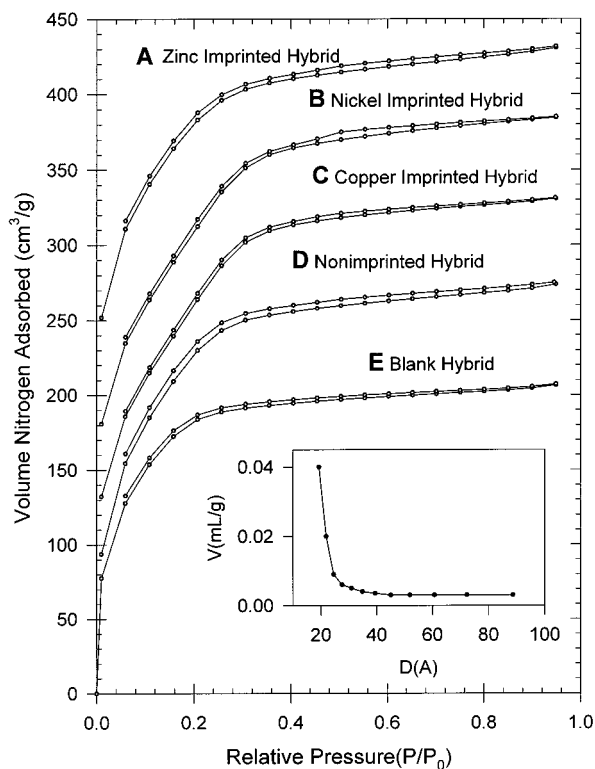


**Figure 9.** Nitrogen adsorption isotherms for imprinted, nonimprinted, and blank hybrid sorbents. Nitrogen volume is the standard temperature and pressure equivalent.  $P/P_0$  is the ratio between the pressure at which the nitrogen was adsorbed and atmospheric pressure.

**Table 5. Surface Areas and Pore Volumes**

sample	BET surface area (m <sup>2</sup> /g)	total pore vol (cm <sup>3</sup> /g)	micropore area (m <sup>2</sup> /g)	micropore vol (cm <sup>3</sup> /g)
blank	600	0.32	475	0.22
nonimprinted	826	0.43	593	0.26
Cu(II) imprinted	823	0.43	473	0.18
Ni(II) imprinted	821	0.44	454	0.17
Zn(II) imprinted	802	0.43	564	0.25

of these sorbents, along with the similar  $d$  spacings of the as-synthesized and extracted materials gives evidence that the surfactant molecules formed assemblies with diameters in the high microporous range (10–20 Å). In addition to these samples, a nitrogen adsorption analysis was performed on an as-synthesized sample (blank as-synthesized). It exhibited a BET surface area of 0.3 m<sup>2</sup>/g and a total pore volume of only 0.002 cm<sup>3</sup>/g. These results clearly indicate the important role of surfactant assemblies in creating porosity in these materials.

**UV-Visible Spectroscopy.** Amine complexes of Cu(II) are more intensely blue than the hydrated cation. The stronger ligand field produced by amines cause the absorption bands of the electronic spectra to shift to shorter wavelengths.<sup>33</sup> This characteristic of copper amine complexes, coupled with relatively large extinction coefficients, has allowed us to probe the nature of the imprinting effect in the copper imprinted sorbents via UV-visible spectroscopy. Since a 1:2 Cu(II) to the (TMS)en complex was formed prior to polymerization and incorporated into the sorbent by copolymerization of BTSE and (TMS)en, the ethylenediamine moieties are

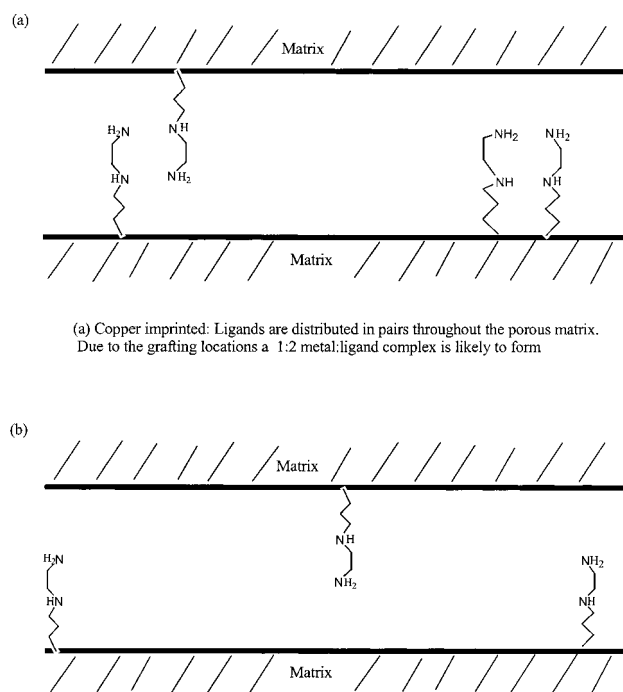


**Figure 10.** Probable arrangement of (TMS)en ligands within pores of imprinted and nonimprinted hybrid sorbents.

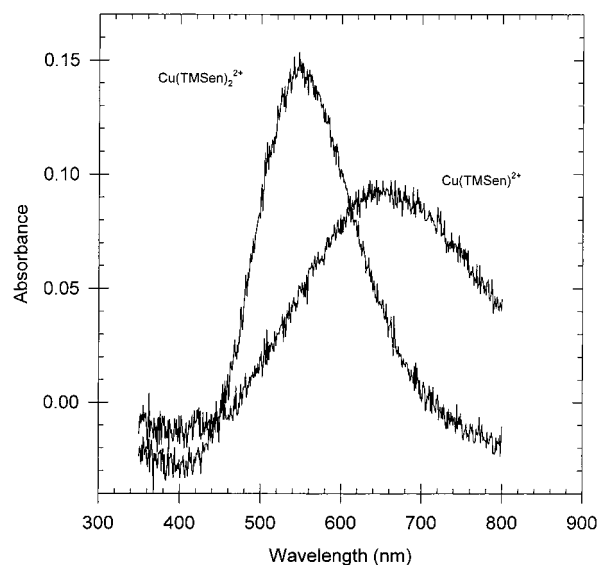


**Figure 11.** UV-vis absorption spectra of (a)  $\text{Cu}((\text{TMS})\text{en})_2^{2+}$  and (b)  $\text{Cu}((\text{TMS})\text{en})^{2+}$  complexes in ethanol.

thought to be “paired up”. Following the removal of the metal ion and surfactant molecules, the (TMS)en ligands are grafted close enough throughout the organic-inorganic matrix that a 1:2 complex is likely to form (Figure 10a). In contrast to this, in the nonimprinted sorbent, the (TMS)en ligands are believed to be homogeneously distributed. This would result in the ligands being too far apart to form the 1:2 complex (Figure 10b). The relatively large stability constant associated with the addition of a second diamine moiety to metal ions<sup>45</sup> would give the copper imprinted material a much higher affinity for Cu(II). Figure 11 shows the solution spectra of  $[\text{Cu}(\text{TMS})\text{en}(\text{H}_2\text{O})_4]^{2+}$  ( $\lambda_{\text{max}} = 651 \text{ nm}$ ), and  $[\text{Cu}$

(45) Smith, R. M.; Martell, A. E. *Critical Stability Constants*; Plenum: New York, 1975; Vol. 2.



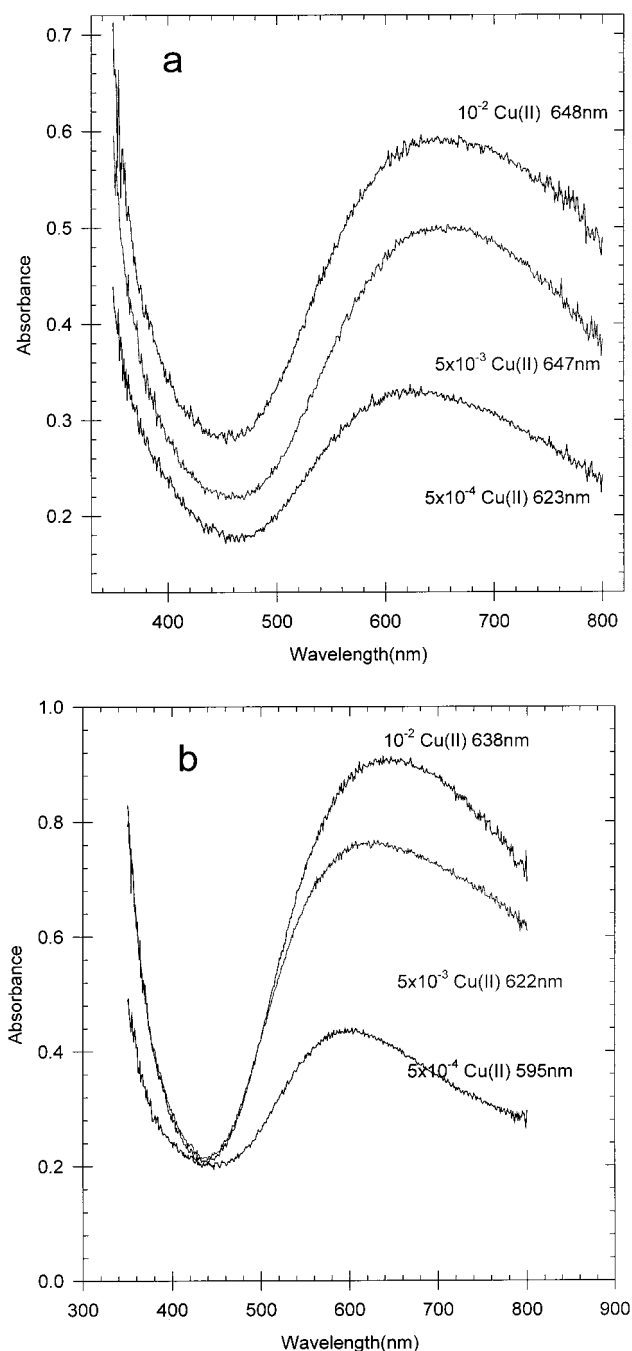


**Figure 12.** UV-vis diffuse reflectance spectra of reloaded (a) nonimprinted and (b) imprinted hybrid sorbents.

(TMS)en<sub>2</sub>(H<sub>2</sub>O)<sub>2</sub><sup>2+</sup> ( $\lambda_{\max}$  = 547 nm). The wavelength shift of 104 nm clearly illustrates the ligand field effect. Batch tests were run with the nonimprinted and copper imprinted sorbents using a Cu(II) solution of  $5 \times 10^{-4}$  M. Diffuse reflectance spectra of the loaded sorbents were then recorded.

**Nonimprinted Hybrid.** Figure 12a shows the electronic spectra of the copper-loaded nonimprinted material. As seen from Figure 12a, the  $\lambda_{\max}$  is 623 nm. This value is close to the value recorded for the 1:1 complex in solution (651 nm). Since the electronic spectra represent the overall distribution of coordination environments, it can be inferred from these results that the nonimprinted material formed only a small percentage of 1:2 complexes at the lower concentration and nearly all 1:1 complexes at the higher two concentrations.

**Copper Imprinted Hybrid.** As seen from Figure 12b, the  $\lambda_{\max}$  for the reloaded imprinted sorbent shifts to 595 nm. This indicates that approximately half of Cu(II) is bound to the imprinted sorbent as a 1:2 complex. The difference in  $\lambda_{\max}$  values of 28 nm for the copper loaded nonimprinted and copper imprinted sorbents using  $5 \times 10^{-4}$  M Cu(II) solutions shows that the imprinted material does in fact bind more copper ions in a 1:2 ratio.

**<sup>13</sup>C NMR Analysis.** Conventional <sup>1</sup>H-<sup>13</sup>C cross-polarization and magic angle spinning (CP/MAS) experiments were used with a proton radio frequency field of 50 kHz for <sup>1</sup>H excitation, spin lock, and dipolar decoupling. The CP contact time was 2.5 ms for all samples. Free induction decays (1K data points, 15 kHz spectral width) were acquired using quadrature detection, zero filled to 8K and smoothed (10 Hz, 0.4 ppm line broadening): carbon chemical shifts are expressed on the tetramethylsilane (TMS) scale ([TMS] = 0 ppm); the methyl chemical shift of hexamethylbenzene = 17.3 ppm) was used as a secondary chemical shift reference. The dominant spectral feature of the solid-state <sup>13</sup>C NMR spectrum of the mesoporous inorganic/organic hybrid network obtained from polymerization of 1,2-bis(triethoxysilyl)ethane (BTSE) is a resonance at 6 ppm for the framework disilylethanyl moiety. The spectrum is similar to that reported by Melde et al.<sup>20</sup> The spectra of all preparations show an sp<sup>2</sup> carbon resonance at 146 ppm assigned to the disilylethanyl analogue of the polymer that is present at 2–3%. This material is derived from 1,2-bis(triethoxysilyl)ethane which is a 2–3% contaminant in the BTSE reagent. Resonances for ethanol (59 and 18 ppm) are in all preparations. The ethanol is not eliminated by extended high vacuum (50  $\mu$ m) pumping cycles. The carbon resonances of the ligand incorporated into the hybrid by copolymerization with (TMS)en are expected at 52, 40, 23, and 11 ppm.<sup>46</sup> The silylmethylene resonance of the ligand (11 ppm) is not resolved from the polymer framework resonance. The extent of (TMS)en bonding in these materials was assessed from integration of the doubly degenerate resonance at 52 ppm representing the two secondary amine carbons in the ligand relative to the framework disilylethanyl resonance. This evaluation shows that the ligand in the nonimprinted hybrid is present at 2 mol %. In like fashion, integration of the Cu imprinted hybrid spectra shows the ligand to be incorporated at the level of 7 mol %. From stoichiometry the maximum ligand concentration is 15 mol %. This solid-state NMR result further supports the advantage of the use of metal ion templates in synthesis of the functionalized hybrid sorbents for not only control of ligand distribution but also increasing the overall ligand concentration in the matrices.

## Conclusions

The key results presented here demonstrate that periodic mesoporous organosilicas can be further functionalized for selective ionic recognition. The formation of coordination complexes between the bifunctional organosilane, (TMS)en, and divalent cations of copper,

(46) Yang, J. Y.; El-Nahhal, I. M.; Chuang, I.-S.; Maciel, G. E. *J. Non-Cryst. Solids* **1997**, *209*, 19–39.

nickel, or zinc and their subsequent incorporation into the polysilsesquioxane framework gives the resulting polymer unique properties. Removal of the metal ions creates cavities within the material with selective rebinding characteristics. These imprinted sorbents exhibit not only a better selectivity but also a higher capacity for the metal ion templates than the non-imprinted analogues. In the case of nickel and zinc imprinted sorbents at pH 6.0, metal ion imprinting has been utilized to synthesize sorbents made of identical materials that preferentially sequester different metal ions (the metal ion template) during competitive ion binding batch tests. In addition, the imprinted polysilsesquioxanes contain more than three times the functional ligands the nonimprinted materials synthesized under similar conditions contain. These materials exhibit excellent metal ion adsorption kinetics, removing >99% Cu(II) from 30 ppm solutions in 60 s. Sorbent regeneration is accomplished by washing in dilute acid. Efficient separations are also exhibited after multiple use cycles. (TMS)<sub>n</sub> has been incorporated into these materials without the decrease in surface area and porosity normally exhibited by MCM-41 silicas upon

addition of organosilanes. This opens up new possibilities for applications of these materials as hosts when a relatively high degree of functionalization and ordered, porous structures are required.

**Acknowledgment.** The authors want to thank Dr. D. A. Loy at the Sandia National Laboratory for helpful discussions and for providing us with purified BTSE for NMR studies. This work was conducted at the Oak Ridge National Laboratory and supported by the Division of Chemical Sciences, Office of Basic Energy Sciences, U.S. Department of Energy, under Contract No. DE-AC05-00OR22725 with UT-Battelle, LLC, and the Environmental Management Science Program (EMSP), U.S. Department of Energy, under Contract No. DE-FG07-97ER14817, between the University of Tennessee and Oak Ridge National Laboratory.

**Supporting Information Available:** Figures showing log  $K_d$  vs metal ion concentration for nickel and zinc imprinted hybrids (PDF). This material is available free of charge via the Internet at <http://pubs.acs.org>.

CM000894M